OPTOELECTRONICS AND ADVANCED MATERIALS – RAPID COMMUNICATIONS Vol. 2, No. 3, March 2008, p. 153 - 160

Characterization of metal nanolayers sputtered on poly(ethyleneterephtalate)

P. SLEPIČKA[a,*], V. ŠVORČÍK[a], M. ŠLOUF[b], V. RYBKA[a], M. ŠPIRKOVÁ[b]
[a]*Department of Solid State Engineering, Institute of Chemical Technology, 166 28 Prague, Czech Republic*
[b]*Institute of Macromolecular Chemistry, Academy of Sciences of the Czech Republic, 162 06 Prague, Czech Republic*

Gold, silver, palladium and platinum layers were sputtered on polyethyleneterephtalate (PET) films. Sheet electrical resistance, surface topography and thickness of this nanolayers were studied by two-point technique, atomic force microscopy, scanning electron microscopy, transmission electron microscopy and atomic absorption spectroscopy. Chemical structure of metal layers was studied by X-ray photoelectron spectroscopy. Resistance of Au and Ag decreased rapidly with the formation of the continuous layer. In case of Pt and Pd this decrease was more gradual. Ag sputtered layer was oxidized. Different surface topography of layer was observed. Au and Pt layers contains worm-like structures, while Ag consists of clusters and Pd forms homogeneous layer with globe clusters. Transmission electron microscopy showed different thicknesses of the continuous metal layers sputtered under the same deposition conditions. When the metal layers are formed, the main role has the nucleation instead of sputtering yield.

(Received 25 February 2008; accepted March 13, 2008)

Keywords: Poly(ethyleneterephtalate), Sputtering, Metal nanolayers, Topography, Chemical structure, Sheet resistance

1. Introduction

Research in the field of nanolayers is a multidisciplinary effort that involves interaction between researchers in the field of physics, chemistry, mechanics and material science, or even biology and medicine. It has been stimulated by the interest for basic scientific investigations and their potential technological applications (e.g. electronics, biomaterials, food packaging).

Metallized polymers are commonly used e.g. for audio- and videorecording tapes, film capacitors, LCD displays [1], light-emitting diodes, polymer film waveguides [2], microchips for isotachophoresis [3], biosensors [4], food and pharmaceutical applications [5], gas barrier applications [6]. Physical vapor deposition (PVD) is a versatile method of synthesis of thin films with structural control at the atomic or nanometer scale by careful monitoring the processing conditions [7-9]. In sputtering, atoms are ejected from the target surface by the impact of energetic ions. Metal films can be prepared on various polymers, e.g. PMMA [3], PET [4,6,10]. Different metals can be used, e.g. Ag [2,10], Au [4,11-13], Al [2,14], Pd [15] or Pt [3,16,17].

For growth of metal film on polymers it is necessary to know morphological and chemical properties of the films [6]. Discontinuous thin films of noble or refractory metals (Au, Ag, Pt, Pd, W, Mo) are readily formed in the "early" stages of nucleation and growth on insulating substrates [18]. Weak atom-substrate interaction is a key element. The films consist of discrete metal islands, of dimension in the 2-10 nm range, separated by inter-island gaps 2 nm or more wide [18]. These typical parameters can differ considerably for particular metal-substrate systems and deposition parameters (e.g. temperature, power). To the growth of metal layers on polymer substrates has been devoted several studies of Faupel et al. [19-22] and the growth on modified polymers has been studied e.g. in work [23,24].

This work is focused on characterization of Au, Ag, Pt and Pd layers sputtered on PET. These metals were chosen since they are close in periodic table of elements. Surface topography was studied using atomic force microscopy (AFM), scanning electron microscopy (SEM); topography in section and the layer thickness was studied by transmission electron microscopy (TEM); continuity of layers and theirs thickness was characterized by measuring electrical sheet resistance; chemical composition of deposited layers was determined by the X-ray photoelectron spectroscopy (XPS).

2. Experimental

2.1. Materials and metal layers deposition

Gold, silver, platinum and palladium (purity 99.99%, supplied by Goodfelow Ltd.) layers were deposited onto 50 μm thick poly(ethyleneterephtalate) (PET, T_m=260 °C, T_g~80 °C), supplied by Goodfellow Ltd. and Si (100) from standard targets by diode sputtering on BAL-TEC, SCD 050 device. Deposition parameters were: room deposition temperature, deposition time 0-300 s, total argon pressure about 4 Pa, the electrode distance of 50 mm, current of 20 mA and discharge voltage 330 V.

2.2. Analytical methods

The continuity of a metal layer was examined by measuring electrical sheet resistance. For determination of

sheet resistance by a standard two-point technique using KEITHLEY 487 pico-ampermeter. For the measurement two Au contact, about 50 nm thick were deposited on the layer surface by sputtering. Typical error of the sheet resistance measurement was ±5%.

The surface topography of pristine PET and deposited metal layers was examined using AFM (contact mode) with Digital Instruments NanoScopeTM Dimension III engine. Olympus oxide-sharpened silicon nitride probes OMCL TR with the spring constant 0.02 N/m was chosen. The normal force of the tip on the sample surface did not exceed 10 nN. Thickness of Au layer, deposited under the same conditions on Si substrate, was measured with AFM. The scratch was made on the metal layers prepared on Si substrate. The scratch depth was measured on five different places.

Chemical structure of metal layers was determined from X-ray photoelectron spectra (XPS), measured on Omicron Nanotechnology ESCAProbeP spectrometer. X-ray source was monochromated at 1486.7 eV and area 2×3 mm^2 was exposed and analyzed. Spectra were measured stepwise with step in binding energy 0.05 eV. The spectra evaluation was carried out by CasaXPS program. Before the measurement the samples were stored under standard laboratory conditions.

The thickness of deposited metal layers up to 130 s was determined by means of atomic absorption spectroscopy (AAS) on a Varian AA 880 device using a flame-atomization technique at 242.8 nm wavelength. From metal concentration the mean layer thickness was determined with a typical uncertainty of ± 5% [11].

Thickness profile was determined also by means of transmission electron microscopy (TEM). Specimens for TEM were cut from the centre of the PET foils with metal layers and fixed in epoxy resin (Durcupan). Ultrathin cross-sections (ca 60 nm) were prepared with ultramicrotome Ultracut UCT (Leica) at room temperature, transferred to TEM microscopy grids and observed in TEM microscope JEM 200 CX (JEOL) at accelerating voltage of 100 kV.

Surface morphology was studied by scanning electron microscopy (SEM), using a field-emission gun equipped SEM microscope Quanta 200 FEG (FEI). Specimens for SEM were also cut from the centre of the PET foils as in the case of TEM microscopy, but the metallic layer was observed from the top. All micrographs were taken with secondary electrons detector in high-vacuum mode at accelerating voltage 30 kV.

3. Results and discussion

3.1. Continuity and chemical structure of metal layers

Layer continuity was characterized by measuring electrical sheet resistance (R_s) [11]. The sheet resistance as a function of the layer thickness for Au, Ag, Pt and Pd is shown in Fig. 1. It is seen that there is a difference in the dependence of sheet resistance on layer thickness for each of metals. For layer thickness up to 4.1 nm (Au) and 2.1 nm (Ag) the sheet resistance of the layer is the same as for pristine PET. Then the rapid decrease of the resistance is observed. Rapid decrease of the sheet resistance of Ag and Au layers observed for higher thicknesses is probably related to the formation of continuity metal layer which was observed also in work [11]. With increasing layer thickness, the sheet resistance achieve a saturation at approx. 5 nm for of Au and Ag. For still higher thicknesses the resistance remains constant. The evolution of the sheet resistance on Pt and Pd layers is quite different. Decrease of the R_s is observed already after 0.2 nm of layer thickness for Pt and almost immediately after start of sputtering for Pd. In comparison with Ag and Au, the decline of R_s as a function of layer thickness of Pt and Pd layers is slower. The region of constant sheet resistance is achieved at thickness of 3.7 nm. The resistance of Pd and Pt layers is by order of magnitude higher comparing to that of Au and Ag layers. The difference is probably due to higher resistance of Pt and Pd bulk material [25] and possibly also to different structure of deposited layers [26].

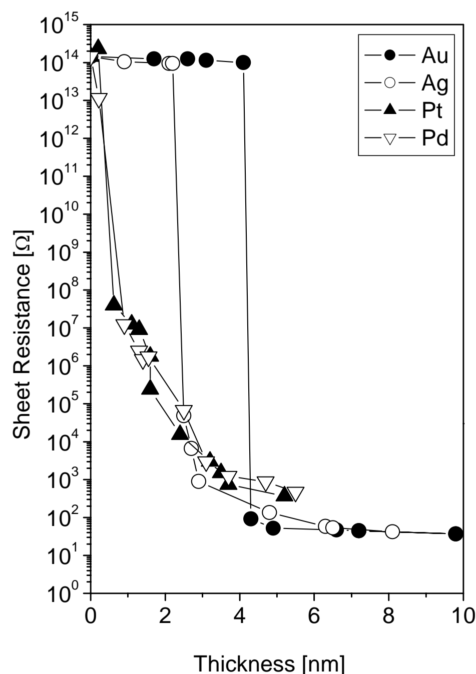

Fig. 1. Dependence of sheet resistance of deposited Au, Ag, Pt and Pd layers on layer thickness. The layers was sputtered on PET.

Chemical structure of metal layers deposited on PET was investigated using XPS technique. The typical XPS spectra are shown in Fig. 2. Maxima for Pt orbitals (4f7/2 a 4f5/2) are at 71.2 and 74.9 eV, for Pd (3d5/2 a 3d3/2) at 335.7 and 341.1 eV and for Au (4f7/2 a 4f5/2) at 83.76 and

87.50 eV. Observed peaks for Au, Pt and Pd correspond to tabular values [27,28]. It may therefore be concluded that the sputtering does not change the chemical structure of the metals. For silver, however, the maximum is shifted to 367.2 eV for oxidized state of silver and 368.3 eV for Ag^0.

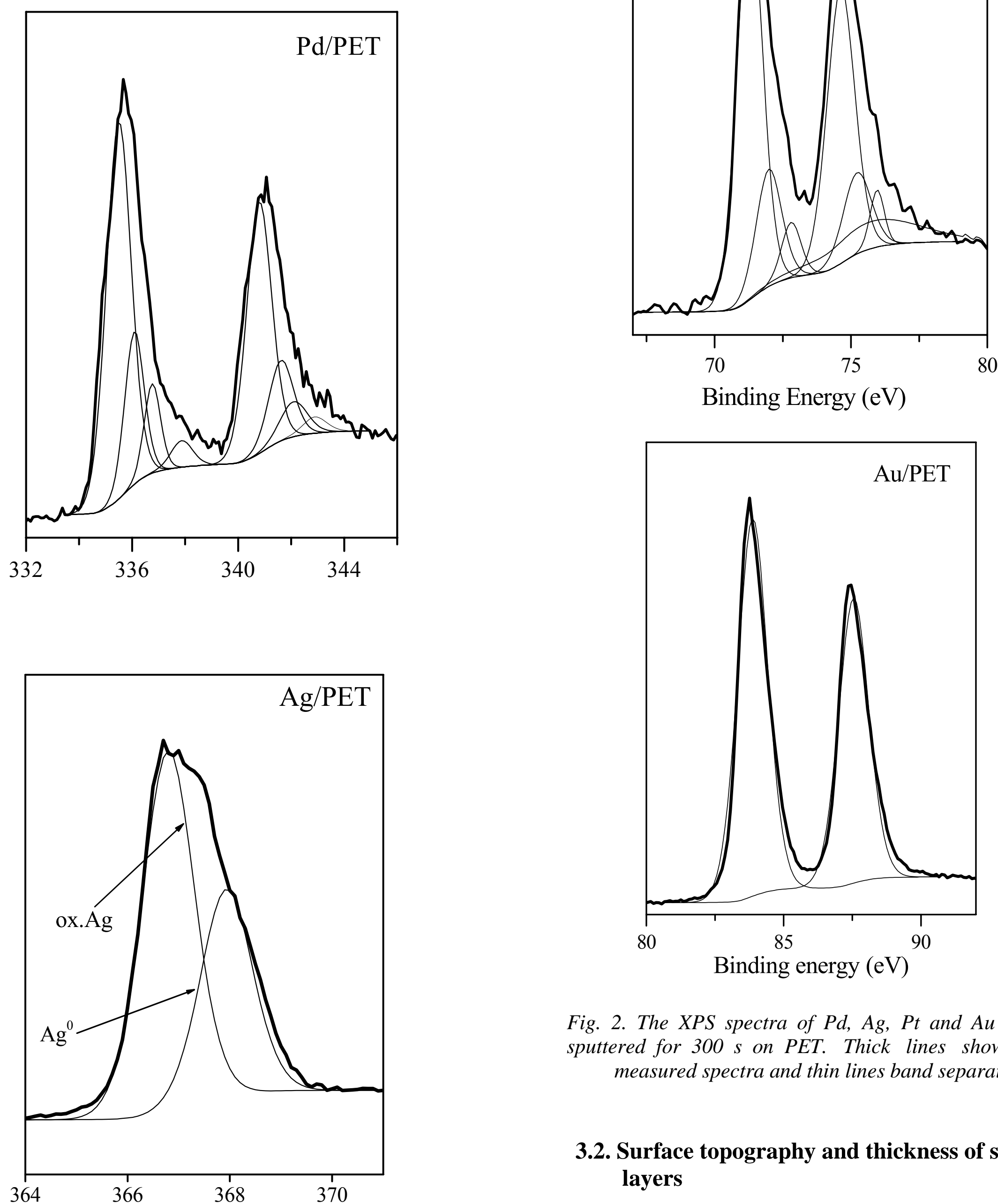

Fig. 2. The XPS spectra of Pd, Ag, Pt and Au layers sputtered for 300 s on PET. Thick lines show the measured spectra and thin lines band separation.

3.2. Surface topography and thickness of sputtered layers

AFM images of surface topography of pristine PET and of early stages (after 10 s deposition) of metal layers on PET are shown in Fig. 3. Pt forms larger clusters in comparison with Pd on the PET surface with surface roughness of R_a 0.59 nm (vs. roughness of Pd 0.27 nm). Au creates small clusters (R_a=0.84 nm) and Ag layer is composed of large clusters in comparison with Au (R_a 0.75 nm).

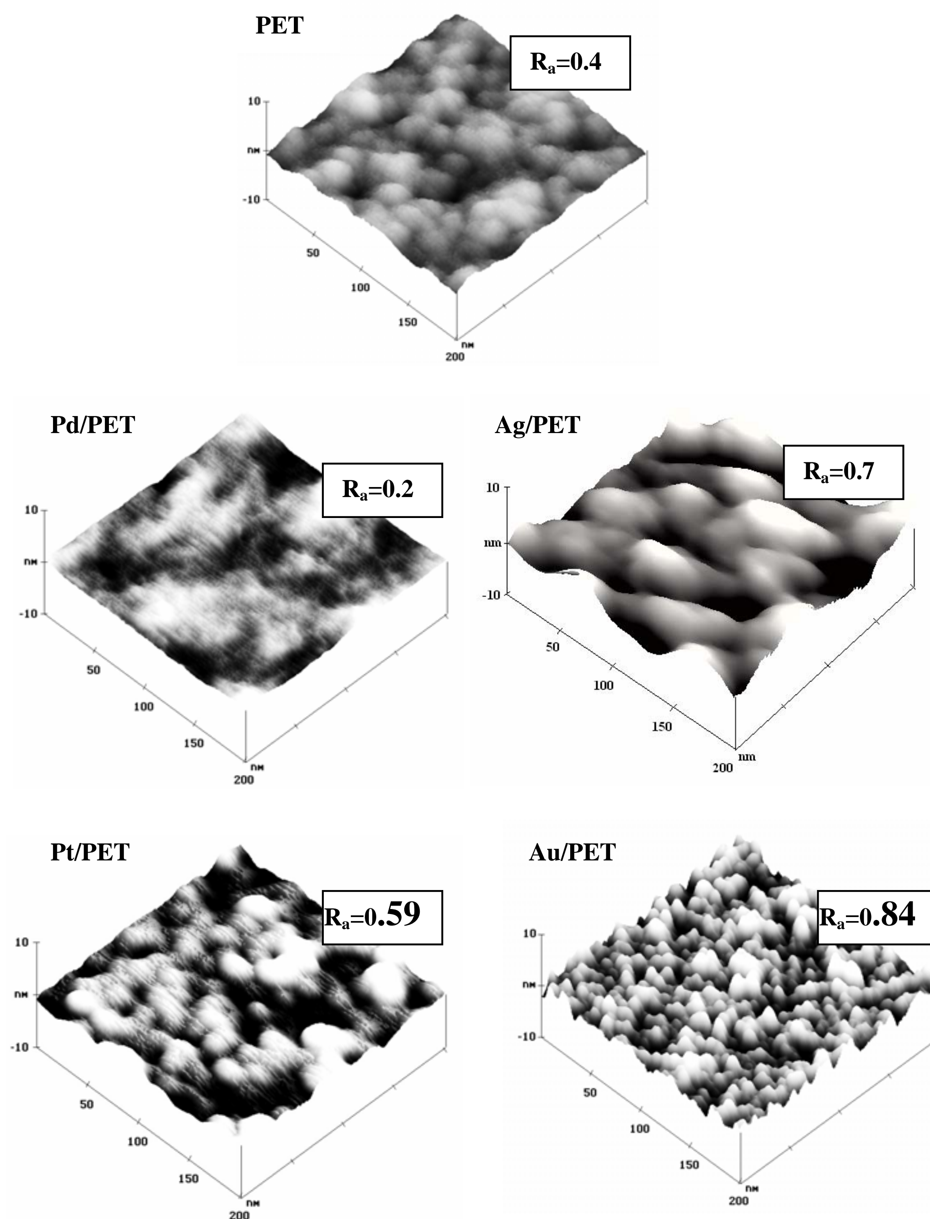

Fig. 3. AFM images of pristine PET and Pd, Ag, Pt and Au layers sputtered for 10 s on PET. R_a is the surface roughness in nm.

Surface topography of PET with discontinuous metal layers (sputtered 25 s) is shown in Fig. 4. The topography and R_a of Pd and Pt layer is most similar to that of sputtered 10 s. Au creates small but sharper clusters (R_a=1.46 nm), the increase of roughness in comparison with layers sputtered with 10 s is observed. Ag layer is composed of round and larger clusters with R_a=1.08 nm. Surface topography of continuous layers is documented in Fig. 5. It is clear that the topography of Pt and Pd layers is quite different from that of Au and Ag layers, the topography of former ones being more similar to that of pristine PET. Ag forms round, large clusters and in Au layers small clusters aggregate into larger and sharper ones.

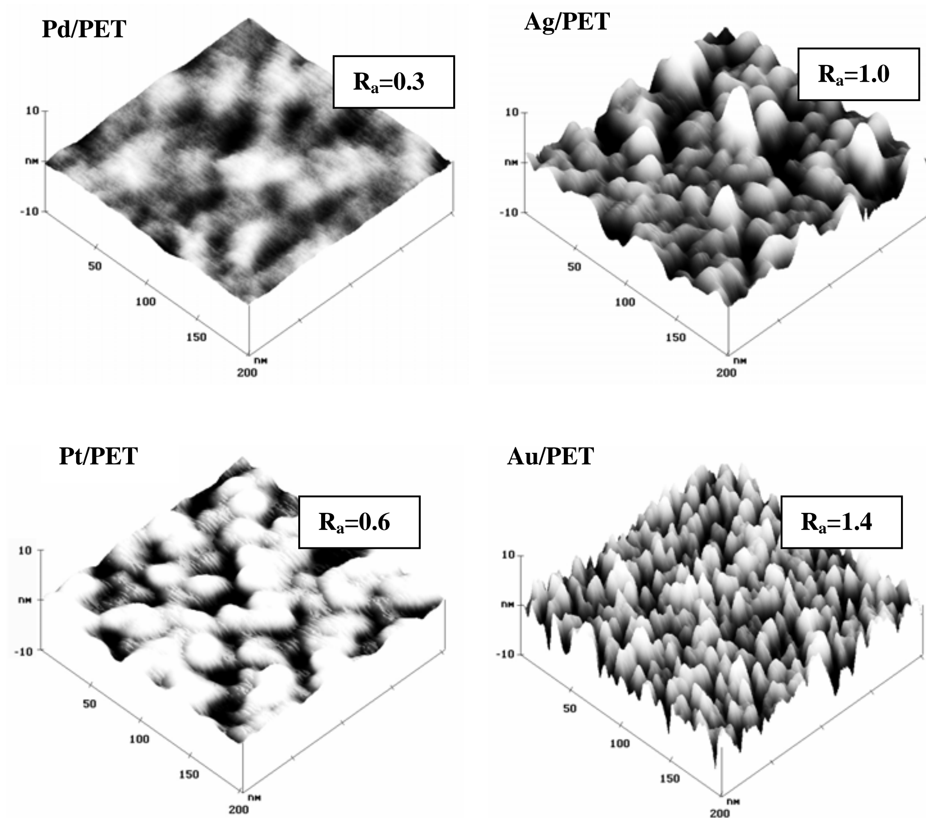

Fig. 4. AFM images of Pd, Ag, Pt and Au layers sputtered for 25 s on PET. R_a is the surface roughness in nm.

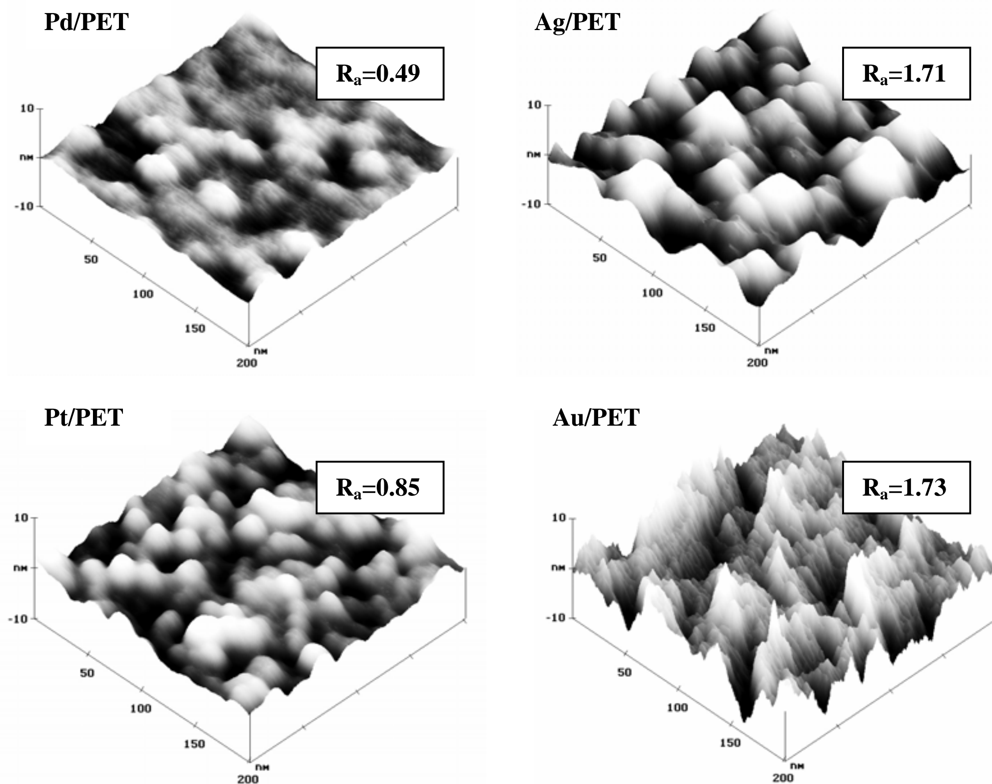

Fig. 5. AFM images of Pd, Ag, Pt and Au layers sputtered 130 s on PET films. R_a is the surface roughness in nm.

In Fig. 6 SEM images of continuous metal layers, prepared by 300 s of sputtering, are shown. Pd layer exhibits the finest surface without any anomalies. On Au and Ag layers a worm-like, heterogeneous structure is observed [12]. For Au layer the heterogeneity is even larger but less frequent. Comparing to other metals Ag exhibits larger spherical clusters.

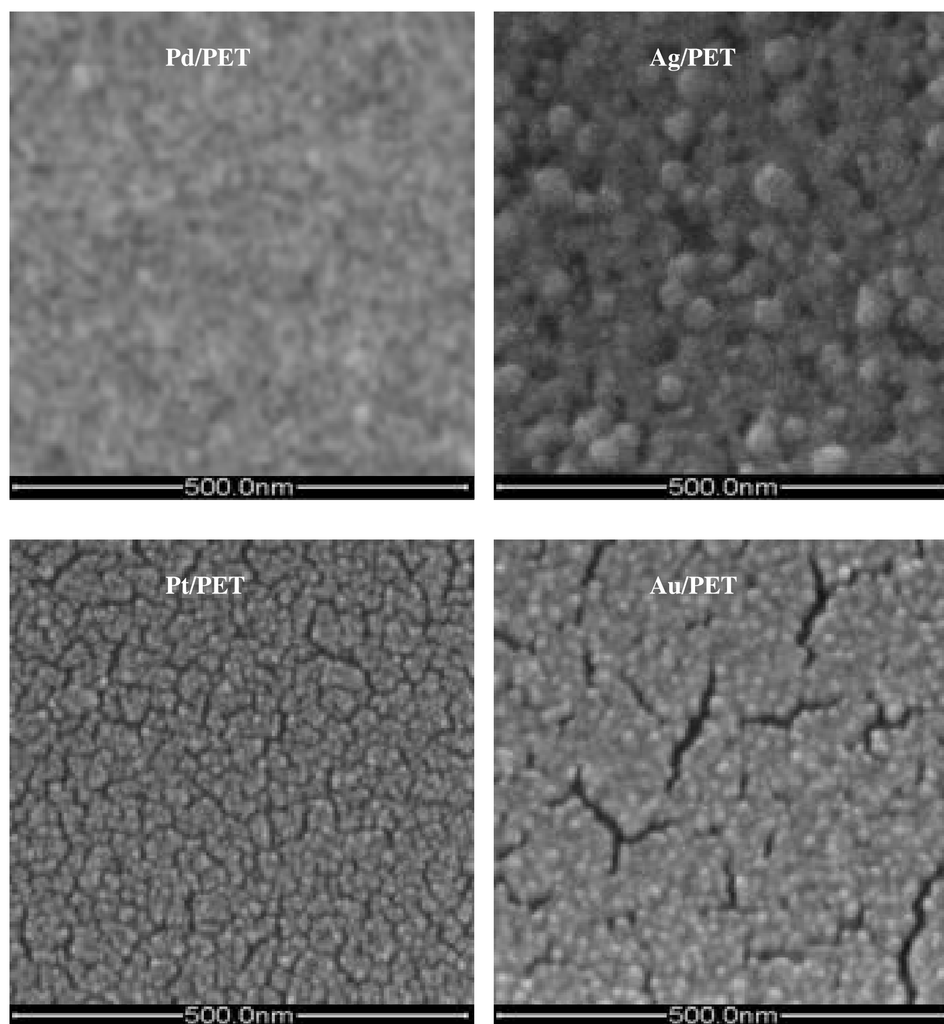

Fig. 6. SEM scans of Pd, Ag, Pt and Au layers sputtered for 300 s on PET films.

The first reason for deposition of metal layers on Si substrate was to study the influence of sputtering yield and substrate on the layer's growth. The thickness of the metal layer can not be determined using AFM method on soft PET since it is impossible to prepare a suitable "scratch", which was the second reason for deposition of metal layers on Si substrate under identical experimental conditions. The thickness measured by AFM technique are summarized in Tab.I together with the values obtained by TEM on the layers deposited on PET (see also Fig. 7). The TEM measurement was performed on very thin cuts obtained from metal-PET composite by ultramicrotome (see above). The thickness was determined from undamaged part of the cut to avoid an error due to possible mechanical deformation taking place in the cut preparation. It is seen from Table 1 that Au and Pt form the layers of similar thickness on PET and Si. The thickness of Ag layer is lower and Pd creates the thinnest layers on both substrates.

Table 1 . Thicknesses of Au, Ag, Pd and Pt layers sputtered for 300 s on Si and PET. Sputtering yields [32] of metals are presented for Ar plasma and 330 eV. The thickness was studied with AFM (on Si) and with TEM (on PET) substrate. TEM values were determined within 15% error.

Metal	**Thickness (nm)**		**Sputtering yield**
	on Si	**on PET**	**(atoms/ion)**
Au	51.6±0.5	73.3	1.53
Ag	41.6±1.4	53.3	2.00
Pd	27.9±1.3	40.0	1.65
Pt	55.6±1.0	66.7	0.94

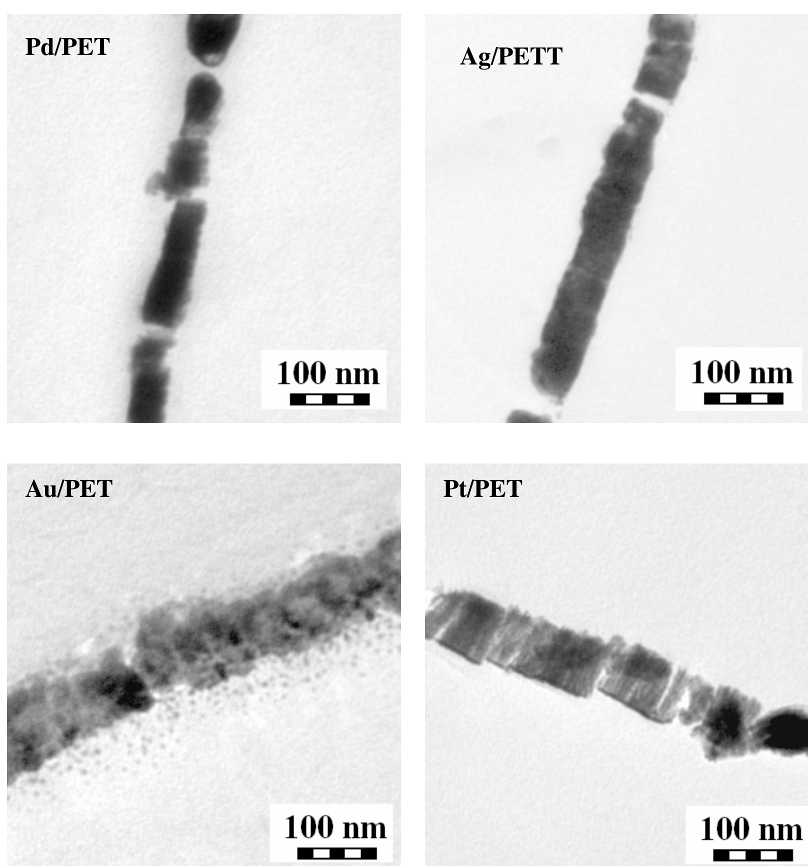

Fig. 7. TEM scans of Pd, Ag, Pt and Au layers sputtered for 300 s on PET films.

Both techniques of thickness measurement (AFM and TEM) give different values of layer thickness on PET and Si. This result can be explained on the basis of current nucleation theory [29-31]. From the theory it follows that the rate of the layer growth is different for sputtering of the same metal on different substrates (e.g Au on PET and Si in the present case) or sputtering of different metal on the same substrate under the same sputtering yield (Au and Pd on Si). For that reason it is possible that the metals with different sputtering yields may form on different substrates the layers with similar thickness. It may be concluded from the present data that the layer thickness is mostly affected by metal nucleation and less by sputtering yields of metals.

4. Conclusions

The thin layers of Au, Ag, Pt and Pd metals deposited onto PET by sputtering technique were characterized by different methods and their electrical resistance was measured as a function of the layer thickness. The transition to continuous layer leads to rapid decrease of the sheet resistance in the case of Au and Ag. The decrease of the sheet resistance of Pt and Pd layers with increasing layer thickness is much slower and the dependence is more complicated. Continuous Au and Ag layers are composed of larger clusters which are sharper for Au and rounder for Ag. Continuous Pt and Pd layers are composed of smaller clusters and their surface topography is similar to that of pristine PET and the values of surface roughness are close. Sputtering does not change the chemical state of metal with only exception of Ag where a metal oxidation is observed in XPS spectra. Worm-like, heterogeneous surface relief is observed on SEM images of continuous Pd and Au layers. On Ag layers round and larger clusters are found. Under the similar deposition conditions on PET and Si substrates, the Au and Pt form the layers of similar thickness which is larger that that from Ag. The thinnest layers are formed by Pd. The observed differences in the thickness of the layers prepared from different metals on the two different substrates can be explained by present nucleation theory. Under the same sputtering conditions the layers of Pt exhibit similar thickness as those of Au, despite of lower sputtering yield of Pt. It may therefore be concluded that the layer thickness on different substrates is mostly affected by metal nucleation on the substrate surface.

Acknowledgements

This work was supported by GA CR under the projects Nos. 102/06/1106 and 204/06/0225, Ministry of Education of the CR under Research program No. 6046137302 and LC 06041 and GAAS CR under the project KAN400480701 and A400500505.

References

[1] J. Y. Kim, D. Sohn, E. R. Kim, Appl. Phys. A **72**, 699 (2001).
[2] S. Wolff, A. R. Giehl, M. Renno, H. Fouckhardt, Appl. Phys. B **73**, 623 (2001).
[3] B. Graß, A. Neyer, M. Jöhnck, D. Siepe, F. Eisenbeiß, G. Weber, R. Hergenröder, Sensor Actuator B **72**, 249 (2001).
[4] Ch. Mayer, R. Palkovits, G. Bauer, T. Schalkhammer J. Nanop. Res. **3**, 361 (2001).
[5] R. J. Narayan, Mater. Sci. Eng. C **25**, 405 (2005).
[6] N. Laidani, R. Bartali, M. Anderle, P. Chiggiato, Diam. Relat. Mater. **14,** 1023 (2005).
[7] S. C. Tjong, H. Chen, Mater. Sci. Eng. R **45**, 1 (2004).
[8] B. Navinšek, P. Panjan, I. Milošev, Surf. Coat. Tech. **116-119**, 476 (1999).
[9] U. Schürmann, H. Takele, V. Zaporojtchenko, F. Faupel, Thin Solid Films **515**, 801 (2006).
[10] S. Fukuda, S. Kawamoto, Z. Gotoh, Thin Solid Films **442**, 117 (2003).
[11] V. Švorčík, J. Zehentner, V. Rybka, P. Slepička, V. Hnatowicz Appl. Phys. A **75**, 541 (2002).
[12] V. Švorčík, V. Rybka, M. Maryška, M. Špírková, J. Zehentner, V.Hnatowicz, Eur. Polym. J. **40**, 211 (2004).
[13] V. Švorčík, V. Kotál, P. Slepička, O. Bláhová, P. Šutta, V. Hnatowicz, Polym Eng Sci **46**, 1326 (2006).
[14] D. Kuhlmeier, E. Rodda, D. N. Furlong, U. Bilitewski, Biosens. Bioelectron. **8**, 925 (2003).
[15] H. Klauk, J. R. Huang, J. A. Nichols, T. N. Jackson, Thin Solid Films **366**, 272 (2000).
[16] R. O'Hayre, S. J. Lee, S. W. Cha, F. B. Prinz, J. Power Sources **109**, 483 (2002).
[17] C. R. K. Rao, D. C. Trivedi, Coordin. Chem. Rev. **249**, 613 (2005).
[18] J. E. Morris Vacuum **50**, 107 (1998).
[19] V. Zaporojtchenko, J. Zekonyte, U. Schuermann, F. Faupel, Nucl. Instrum. Meth. B **236,** 95 (2005).
[20] V. Zaporojtchenko, J. Zekonyte, A. Biswas, F. Faupel, Surf. Sci. **532-535,** 300 (2003).
[31] V. Zaporojtchenko, K. Behnke, T. Strunskus, F. Faupel, Surf. Sci. **454-456**, 412 (2000).
[32] V. Zaporojtchenko, K. Behnke, A. Thran, T. Strunskus, F. Faupel, Appl. Surf. Sci. **144**, 355 (1999).
[33] V. Švorčík, J. Siegel, P. Slepička, V. Kotál, M. Špírkovám, Surf. Interf. Anal. **39**, 79 (2007).
[34] V. Kotál, V. Švorčík, P. Slepička, O. Bláhová, P. Šutta, V. Hnatowicz, Plasma Proc. Polym. **4,** 69 (2007).
[35]http://www.goodfellow.com/scripts/web.wl?MGWLPN=MNT&PROG=GOTOSTAT&LAN=E&CTRY=720, 30.1.2008.
[36] M. Fahland, P. Karlsson, C. Charton, Thin Solid Films **392**, 334 (2001).
[37] B.Vincent Crist In: Handbooks of Monochromatic XPS Spectra– The Elements and Native Oxides, XPS International LLC, (2004).
[38] http://www.xpsdata.com, 30.1.2008.
[39] D. Walton, J. Chem. Phys. **37**, 2182 (1962).
[40] D. Walton, Phil Mag **7**, 1671 (1962).
[41] D. Walton, T. N. Rhodin, R. W. Rollins, J. Chem. Phys. **38,** 2698 (1963).
[42] http://www.npl.co.uk/nanoanalysis/arsputtergroups. pdf, 12.5.2007.

*Corresponding author: petr.slepicka@vscht.cz